A Shoreline Evolution Model With the Wavelength Effect of Breaking Waves on Groin Structures

Pidok Unyapoti, Nopparat Pochai

Abstract— **Local sea level rise, strong wave action, and tidal currents all wear down or carry away rocks, soil, and sand along the beaches. The quantity of beach areas has decreased as a result of this issue. Analyzing the progression of the shoreline can help us better understand how the beach will look in the future. A groin structure was built to stop beach erosion and repair the beach. Beach erosion and beach deposition research requires a qualitative analysis of the model shoreline behavior in connection to the governing process. Models for shoreline evolution are the subject of some research. However, they focus on the shoreline evolution in an area between a couple of groin structures. The investigated area of shoreline evolution with a pair of groin structures is enlarged in this research to include the groin system and surrounding area. A more realistic shoreline evolution model has been presented, which takes into account the wavelength influence of breaking waves on groin constructions. The initial condition setting approach and boundary conditions techniques, as well as various groin structural impacts, are discussed. A wave crest impact model and five wavelength effects of breaking waves are introduced. Each year, the coastline evolution is approximated using the classical forward-time centered-space method and the unconditionally stable Saulyev finite differential methods. The estimated impacts of shoreline evolution were consistent with the wave crest impact model for five case wavelengths. For assessing long coastline evolution, the numerical models presented enable a reasonable simulation. The efficiency of building a groin system on a nearby beach might be predicted using the proposed modeling.**

Index Terms—**shoreline evolution, groin system, explicit finite method, wave crest impact, mathematical model**

I. Introduction

Beach erosion is a natural process by which local sea-level rise, strong wave action, and coastal flooding wear down or carry away rocks, soils, and sands along the beach. In many countries, beach erosion is responsible for coastal property loss, including damage to structures and loss of land. This is a problem that causes a decrease in beach areas. A groin structure was invented to prevent beach erosion and thus restore the beach. In [1], they proposed a new method to practical groin modeling, which is explained through the use of the GENESIS shoreline response model to examine the effect of single and multiple groins. The study's predictions are put to test in the replication of the shoreline modification observed in the groin area of Westhampton, Long Island, New York. In [2], They presented groynes-constructed coir geotextiles in the shape of cocologs, as well as the effects of positioning groynes at various angles to determine the most capable setting for minimizing erosion. The results show that a groyne angle of 1350 provides the best protection.

Many authors have developed one-line theory, and several contributors to the analytical solution of the evolution of the shoreline include [3], [4], [5], [6], [7], [8], and [9]. Analytical solutions are usually useful for providing qualitative insight and comprehending the characteristics of long-term shoreline modification. However, analytical solutions have limitations. A numerical method of shoreline evolution may be more relevant for the actual scenario than an analytical solution because an analytical solution cannot be anticipated to tackle problems with complicated boundary conditions and wave inputs.

In [12], they presented a comparison of analytical solutions and two numerical techniques of shoreline evolution under idealized wave conditions for two case shoreline scenarios. The two numerical methods are Forward Time Centered Space techniques and Backward Time Centered Space techniques. The results show that Backward Time Centered Space techniques are more appropriate than Forward Time Centered Space techniques for simulating long-term shoreline change. In [13], [14], [15], [16], [17], and [32], they approximated their model solutions using conditionally stable explicit finite difference methods. In [18], [19], [20], [21], [33], and [34], they approximated their model solution using numerical approaches. In [30], they introduced shoreline evolution when a couple of groins were added. They use two numerical methods to develop shoreline evolution. The first numerical method is the classic forward time-centered space method. The second numerical method is the unconditionally stable Saulyev finite difference methods.

In [22], the purpose of this research is to generate a practical, universal, and replicable chain approach that can aid in comprehensively understanding the dynamics of a coastal system, identifying typical and recurring erosion-accretion processes, and prediction likely future trends relevant to coastal activity planning. In [23], they proposed a

Manuscript received February 25, 2022; revised June 23, 2022.

This paper is supported by Centre of Excellence in Mathematics, Ministry of Higher Education, Science, Research and Innovation, Bangkok, Thailand.

N. Pochai is an Assistant Professor of Department of Mathematics, Faculty of Science, King Mongkut's Institute of Technology Ladkrabang, Bangkok, 10520, Thailand (corresponding author to provide phone: 662-329-8400; fax: 662-329-8400; e-mail: nop_math@yahoo.com).

P. Unyapoti is a PhD. candidate of Mathematics Department, Faculty of Science, King Mongkut's Institute of Technology Ladkrabang, Bangkok, 10520, Thailand (e-mail: pidokunyapoti@gmail.com).

one-line model idea, which has been used to achieve long-term shoreline modeling as well as to aid and generate stronger coastal engineering techniques for managing erosion. The model was tested on Portugal's two northwest coasts, Aveiro and Figueira da Foz. In [24], they proposed using a long-term morphological dataset to morphometrically characterize the evolution of the shoreline along the Holland coast, from Den Helder to Hoek van Holland, and to relate this to the evolution of the complete littoral profile (1964-1992). In [25], they proposed that the research results, in addition to assessing the effects of groins on shoreline modification, serve as a precursor for initiating appropriate mitigation measures to prevent future erosion and instability of the coastline while maintaining the safety and economic design of offshore, coastal, and port structures. In [26], they proposed that the evolution of a beach restoration project in Long Branch, NJ be examined using the empirical orthogonal functions method (EOF). The majority of EOF applications on beach fill projects have been on classic linear fills on generally long, straight, uninterrupted coastlines. The Long Branch project was unusual in that it was conceived as a feeder beach and built within a groin field. In [27], they proposed the comparison of analytical and numerical solutions in the idealized wave condition for four different shoreline situations.

In this research, a shoreline evolution model that takes into consideration the wavelength effect of breaking waves on groin structures is focused. We introduce a governing equation for a one-dimensional shoreline evolution model, initial conditions, and boundary conditions when a couple of groins are added, a wave crest impact model, and five case wavelength effects of breaking waves. Finite difference techniques will be used to approximate the model solution.

II. Governing Equation

A. Shoreline evolution model

In a one-dimensional shoreline evolution model, while maintaining the same shape, the beach shape is supposed to move towards land and towards the sea, meaning that all the bottom outlines become parallel.

As a result of this assumption, the horizontal direction of the baseline profile must be defined, and one contour line should be used to specify changes to the design and volume of the beach plane as the beach erodes and accumulates. The model's main assumption is that sand is transported along the coast on a profile between two well-defined limit elevations. A contribution to the adjustment in volume occurs where there is a discrepancy in the rate of longshore sand transfer on the side of the segment and the related sand consistency. The principles of conservation of mass must be always adapted to the system. The following differential equation for the evolution of the shoreline is generated by considering the above concepts,

$$\frac{\partial y}{\partial t} = \frac{1}{D_B + D_C}\left(-\frac{\partial Q}{\partial x}\right), \tag{1}$$

where x is the co-ordinate on the shores (m), y is the location of the shoreline (m) and perpendicular to the x-axis, t is time (day), Q is the long-shore sand transport rate (m^3/day), D_B is the average height of the berm (m) and D_C is the average depth of closure (m).

To solve (1), it was necessary to define a term for the longshore sand transport rate (Q). This quantity is assumed to have been obtained by the oblique wave occurring to the shoreline. The US Army Corp has created a generalized term for long-shore sand transport rate [10],

$$Q = Q_0 \sin\left(2\alpha_b\right), \tag{2}$$

where Q_0 is the long-shore sand transport rate amplitude. The general formula for the long-shore sand transport rate amplitude is as follows [11],

$$Q_0 = \frac{\rho}{16}\left(H_b^2 c_{gb}\right)\frac{K}{(\rho_s - \rho)(1-n)}, \tag{3}$$

The angle between breaking wave crest impact angle and local shoreline (α_b) can be written as,

$$\alpha_b = \alpha_0 - \tan^{-1}\left(\frac{\partial y}{\partial x}\right), \tag{4}$$

where α_0 is the angle between breaking wave crests impact angle and x-axis. In the case of shoreline with a slight slope, it can be concluded that the angle of the wave breaking to the shoreline is minimal.

Assuming that, $\sin\left(2\alpha_b\right) \approx 2\alpha_b$ and $\tan^{-1}\left(\frac{\partial y}{\partial x}\right) \approx \left(\frac{\partial y}{\partial x}\right)$.

By substituting (4), in (2), and assuming a shoreline with a slight slope, we obtain,

$$Q = Q_0\left(2\alpha_b - 2\frac{\partial y}{\partial x}\right), \tag{5}$$

by substituting (5), in (1), and ignoring the sources or sinks along the shoreline provides the following:

$$\frac{\partial y}{\partial t} = D\frac{\partial^2 y}{\partial x^2}, \tag{6}$$

for all $(x,t) \in (L,T)$, where $D = \frac{2Q_0}{D_B + D_C}$.

B. Physical parameters

The physical parameters of the model are illustrated in Fig. 1-2. which are listed below.

α_0 is the angle between breaking wave crests impact angle and x-axis.

Q_0 is the long-shore sand transport rate amplitude.

D_B is the averaged berm height.

D_C is the averaged closure depth.

L is Alongshore.

T is the Time of simulation.

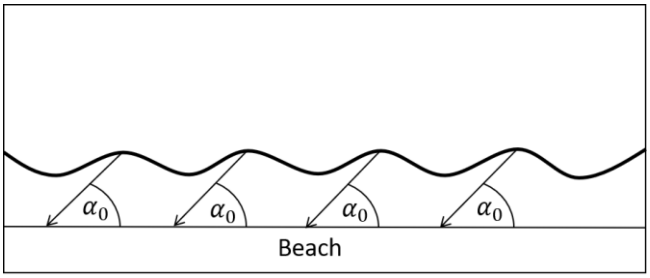

Fig. 1. Breaking wave crests impact angle

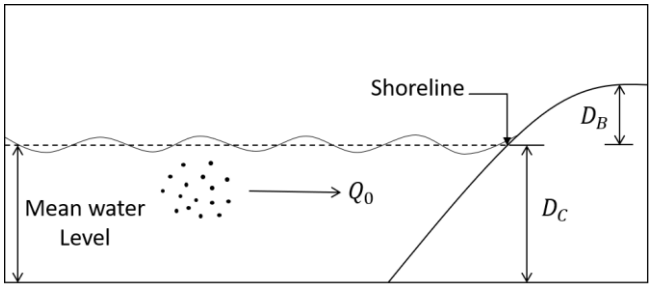

Fig. 2. Shoreline physical parameters

C. The initial and boundary conditions

Straight Impermeable groin system.

The initial shoreline is assumed to be parallel to the x-axis.

Assuming that, the angle between breaking wave crests impact angle to the shoreline is α_0 as shown in Fig. 3. It follows that the sand transport rate along the shoreline is uniform. The groin is added instantly at $x=0$ are illustrated in Fig. 3. These means that the initial condition becomes,

$$y(x,0)=0, \tag{7}$$

boundary conditions are also assumed by,

$$\frac{\partial y(0,t)}{\partial x}=-\tan(\alpha_0) \quad \text{at} \quad x=0, \tag{8}$$

and

$$\frac{\partial y(L,t)}{\partial x}=-\tan(-\alpha_0) \quad \text{at} \quad x=L, \tag{9}$$

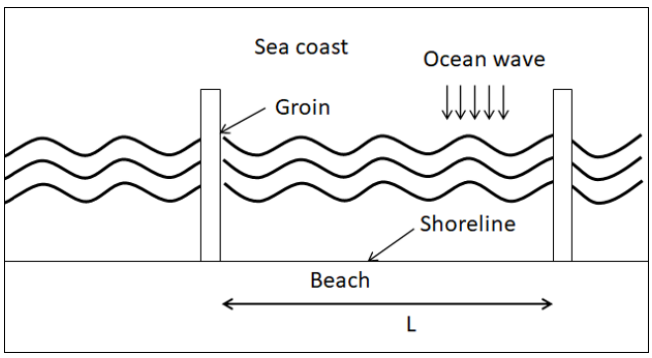

Fig. 3. Initial shoreline with configuration straight impermeable groins.

D. Wave crest impact model

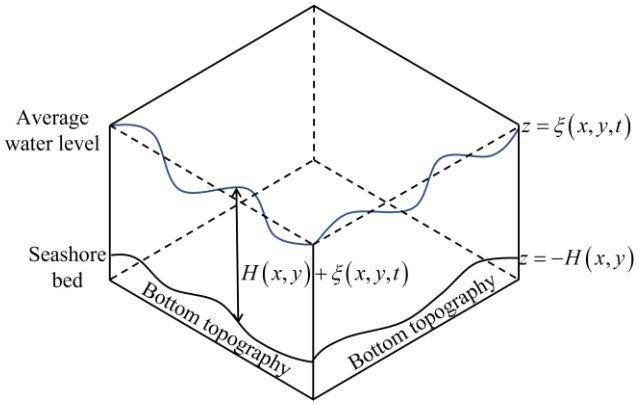

Fig. 4. Water elevation and bottom topography.

The hydrodynamic model is introduced to obtain the wave crest impact in the shoreline evolution model [28].

The two-dimensional unstable water flows into and out of the seashore can be predicted using a system of shallow water equations that account for mass and momentum conservation. The equations of this method should be derived from the vertical direction of the depth-averaging of the Navier-Stokes equations, ignoring momentum diffusion owing to vibration and excluding terms indicating the effects of friction, surface wind, Coriolis factor, and shear stress. The equation of continuity is then expressed as follows:

$$\frac{\partial h}{\partial t}+\frac{\partial(uh)}{\partial x}+\frac{\partial(vh)}{\partial y}=0, \tag{10}$$

and the momentum equations are expressed as below:

$$\frac{\partial(uh)}{\partial t}+\frac{\partial\left(u^2h+\frac{1}{2}gh^2\right)}{\partial x}+\frac{\partial(uvh)}{\partial y}=0, \tag{11}$$

$$\frac{\partial(uh)}{\partial t}+\frac{\partial(uvh)}{\partial x}+\frac{\partial\left(v^2h+\frac{1}{2}gh^2\right)}{\partial y}=0, \tag{12}$$

where

$h(x,y,t)$ is the depth estimated from the average water surface to the seashore bed (m) $h=H+\xi$,

$\xi(x,y,t)$ is the elevation of the water surface from the average water level in the seashore (m),

$H(x,y)$ is the interpolated bottom topography function of the seashore (m),

$u(x,y,t)$ is the velocity in the direction of x (m/s),

$v(x,y,t)$ is the velocity in the direction of y (m/s),

g is a constant of gravity $(9.8\,m/s^2)$.

Such time (t), and two space coordinates, x and y are the independent variables. Likewise, the conserved quantities are mass, which is proportional to h, and momentum, which is proportional to (uh) and (vh). The partial derivatives are grouped into vectors $(\partial x,\partial y,\partial t)$ and

then rewritten as a partial differential hyperbolic equation concerning the same term as follows:

$$U=\begin{pmatrix} h \\ uh \\ vh \end{pmatrix}, F(U)=\begin{pmatrix} uh \\ u^2h+\frac{1}{2}gh^2 \\ uvh \end{pmatrix}, \quad (13)$$

$$G(U)=\begin{pmatrix} vh \\ uvh \\ v^2h+\frac{1}{2}gh^2 \end{pmatrix}, \quad (14)$$

the hyperbolic PDE:

$$\frac{\partial U}{\partial t}+\frac{\partial F(U)}{\partial x}+\frac{\partial G(U)}{\partial y}=0. \quad (15)$$

E. The initial and boundary condition for wave crest impact model

The initial condition of the reservoir was as follows: the x and y velocity components were zero as well as the water elevation: $u=0, v=0$ and $\xi=0$.

Assuming that the breakwater is not a perfect barrier to water as it is made of an aggregate of rocks with large gaps.

The boundary condition was as follows: $(i)\ u=0, \frac{\partial v}{\partial y}=0, \xi=f(x,y,t)$ for wave coming, $(ii)\ \frac{\partial u}{\partial x}=0, \mathrm{v}=0, \frac{\partial \xi}{\partial x}=0$ for left and right boundary, $(iii)\ u=0, \frac{\partial v}{\partial y}=0, \frac{\partial \xi}{\partial y}=0$ for along the beach, $(iv)\ u=0, \frac{\partial v}{\partial y}=0, \frac{\partial \xi}{\partial y}=0$ for top groin structure, and $(v)\ \frac{\partial u}{\partial x}=0, \mathrm{v}=0, \frac{\partial \xi}{\partial x}=0$ for left and right groin structure. The boundary conditions are illustrated in Fig. 5-6.

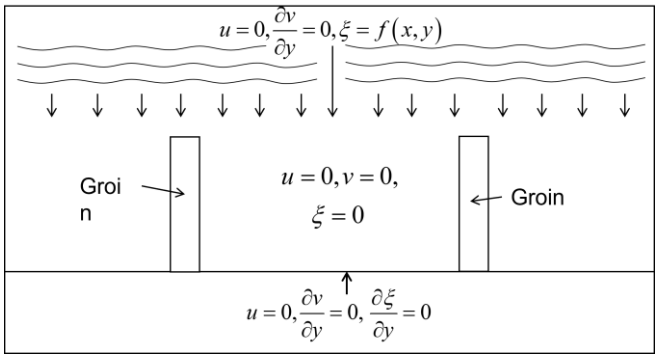

Fig. 5. Initial and boundary conditions.

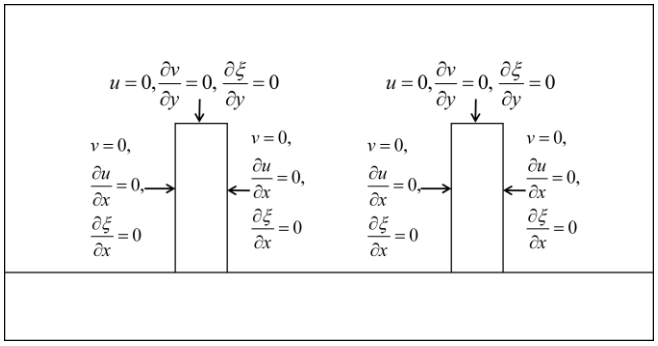

Fig. 6. Initial and boundary conditions for groin structure.

III. Numerical Techniques

A. Grid Spacing

We are discretizing (6) by splitting the interval $[0,L]$ into M subintervals such as $M\Delta x=L$ and the interval $[0,T]$ into N subintervals such as $N\Delta t=T$. We then approximate $y(x_i,t_n)$ by y_i^n, at the point $x_i=i\Delta x$ and $t_n=n\Delta t$, where $0\le i\le M$ and $0\le n\le N$ in which there are positive integers of M and N.

B. Traditional forward time centered space techniques

The forward time centered space techniques will also be used. Consequently, the finite difference approximation becomes [29],

$$y\cong y_i^n, \quad (16)$$

$$\frac{\partial y}{\partial t}\cong\frac{y_i^{n+1}-y_i^n}{\Delta t}, \quad (17)$$

$$\frac{\partial y}{\partial x}\cong\frac{y_{i+1}^n-y_{i-1}^n}{2\Delta x}, \quad (18)$$

$$\frac{\partial^2 y}{\partial x^2}\cong\frac{y_{i+1}^n-2y_i^n+y_{i-1}^n}{(\Delta x)^2}, \quad (19)$$

where $A=\frac{D\Delta t}{(\Delta x)^2}$.

By substituting (16) – (19), in (6), we obtain,

$$\frac{y_i^{n+1}-y_i^n}{\Delta t}=D\left(\frac{y_{i+1}^n-2y_i^n+y_{i-1}^n}{(\Delta x)^2}\right), \quad (20)$$

for $1\le i\le M-1$ and $0\le n\le N-1$. From (20), we get an explicit form of finite difference as follows:

$$y_i^{n+1}=Ay_{i+1}^n+(1-2A)y_i^n+Ay_{i-1}^n, \quad (21)$$

for $1\le i\le M-1$ and $0\le n\le N-1$.

C. An unconditionally Saulyev finite difference techniques

The Saulyev finite difference techniques will also be used. We can obtain that the finite difference approximation is

$$y\cong y_i^n, \quad (22)$$

$$\frac{\partial y}{\partial t} \cong \frac{y_i^{n+1} - y_i^n}{\Delta t}, \tag{23}$$

$$\frac{\partial^2 y}{\partial x^2} \cong \frac{y_{i+1}^n - y_i^n - y_i^{n+1} + y_{i-1}^{n+1}}{(\Delta x)^2}, \tag{24}$$

where $A = \frac{D\Delta t}{(\Delta x)^2}$.

By substituting (22) – (24), in (6), we obtain,

$$\frac{y_i^{n+1} - y_i^n}{\Delta t} = D\left(\frac{y_{i+1}^n - y_i^n - y_i^{n+1} + y_{i-1}^{n+1}}{(\Delta x)^2}\right), \tag{25}$$

for $1 \le i \le M-1$ and $0 \le n \le N-1$. From (25), we get an explicit form of finite difference as follows:

$$y_i^{n+1} = \frac{1}{(1+A)}\left(Ay_{i+1}^n + (1-A)y_i^n + Ay_{i-1}^{n+1}\right), \tag{26}$$

for $1 \le i \le M-1$ and $0 \le n \le N-1$.

D. Numerical techniques for the wave crest impact model

The finite difference technique:

$$U_{i,j}^{n+1} = U_{i,j}^n - \frac{\Delta t}{\Delta x}\left(F_{i+\frac{1}{2},j}^{n+\frac{1}{2}} - F_{i-\frac{1}{2},j}^{n+\frac{1}{2}}\right) - \frac{\Delta t}{\Delta y}\left(G_{i,j+\frac{1}{2}}^{n+\frac{1}{2}} - G_{i,j-\frac{1}{2}}^{n+\frac{1}{2}}\right). \tag{27}$$

E. The wave crest impact

The wave crest impact becomes

$$\alpha(x_i, y_j, t) = \tan^{-1}\left(\frac{v(x_i, y_j, t)}{u(x_i, y_j, t)}\right), \tag{28}$$

the averaged wave crest impact is assumed by

$$\alpha_0(t) = \frac{\sum_{i=1}^{N_P} \alpha(x_i, 0, t)}{N_P}, \tag{29}$$

where N_P is several wave crest impact sample points along the shoreline.

F. The employment of traditional forward time centered space techniques to the left and the right boundary conditions

The forward time centered space techniques will also be used. Consequently, the finite difference approximation becomes,

$$y \cong y_i^n, \tag{30}$$

$$\frac{\partial y}{\partial t} \cong \frac{y_i^{n+1} - y_i^n}{\Delta t}, \tag{31}$$

$$\frac{\partial y}{\partial x} \cong \frac{y_{i+1}^n - y_{i-1}^n}{2\Delta x}, \tag{32}$$

where $A = \frac{D\Delta t}{(\Delta x)^2}$.

By substituting (30) - (32), in (6), we obtain,

$$\frac{y_i^{n+1} - y_i^n}{\Delta t} = D\left(\frac{y_{i+1}^n - 2y_i^n + y_{i-1}^n}{(\Delta x)^2}\right), \tag{33}$$

For i = 0, the substitution of the uncertain value of the left boundary is approximated by the method of center difference with the specified left boundary condition. We obtain,

$$y_{-1}^n = y_1^n - 2(\Delta x)(-\tan(\alpha_0)), \tag{34}$$

by substituting (34), in (33), we obtain,

$$y_i^{n+1} = (1-2A)y_i^n + 2Ay_{i+1}^n - 2A(\Delta x)(-\tan(\alpha_0)), \tag{35}$$

For i = M, the substitution of the uncertain value of the right boundary is approximated by the method of center difference with the specified right boundary condition. We obtain,

$$y_{M+1}^n = y_{M-1}^n + 2(\Delta x)(-\tan(-\alpha_0)), \tag{36}$$

by substituting (36), in (33), we obtain,

$$y_i^{n+1} = 2Ay_{i-1}^n + (1-2A)y_i^n + 2A(\Delta x)(-\tan(-\alpha_0)), \tag{37}$$

(35), and (37), could be used to approximate the values y_i^n of the solution domain grid points.

IV. Wavelength Setting Techniques

The simulation considers alongshore between groin are illustrated in Fig. 7. Table 1 shows the consideration of wavelengths. We assumed waves came in a function of wavelength $0.5\sin(t + \Lambda x)$.

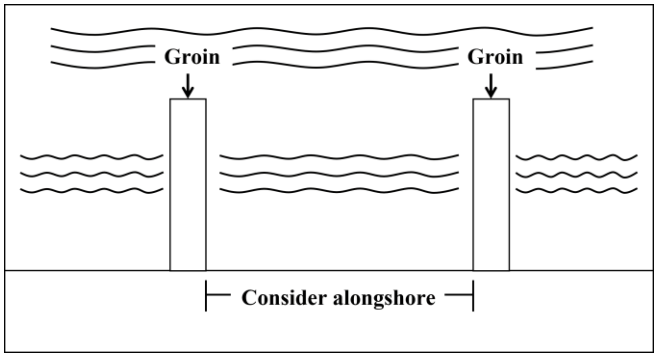

Fig. 7. Consider alongshore.

TABLE I
Wavelength Setting

Simulation	Λ	Wavelength
1	0.01	$0.5\sin(t+0.01x)$
2	0.02	$0.5\sin(t+0.02x)$
3	0.03	$0.5\sin(t+0.03x)$
4	0.04	$0.5\sin(t+0.04x)$
5	0.05	$0.5\sin(t+0.05x)$

We will employ the finite difference techniques to approximate the wave crest impact model solution for wavelengths $0.5\sin(t+0.01x)$, $0.5\sin(t+0.02x)$, $0.5\sin(t+0.03x)$, $0.5\sin(t+0.04x)$ and $0.5\sin(t+0.05x)$. The approximated wave crest impact model solutions for five case wavelengths are illustrated in Fig.8-12. The approximated vector fields of velocities for five case wavelengths are illustrated in Fig. 13-17.

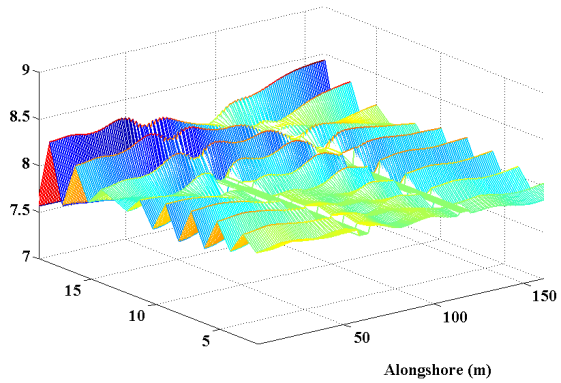

Fig. 8. Wave crest impact in 15 years when wavelength $0.5\sin(t+0.01x)$.

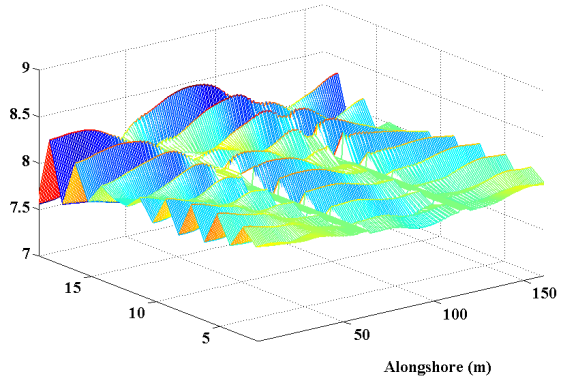

Fig. 9. Wave crest impact in 15 years when wavelength $0.5\sin(t+0.02x)$.

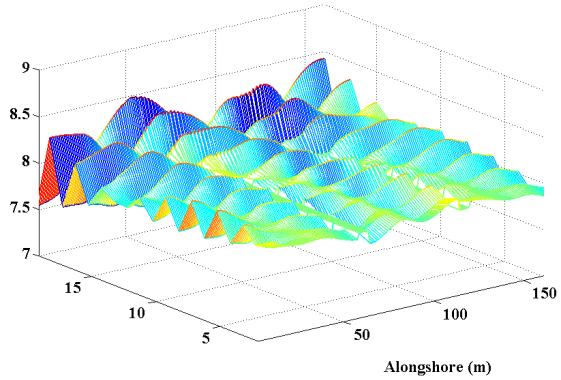

Fig. 10. Wave crest impact in 15 years when wavelength $0.5\sin(t+0.03x)$.

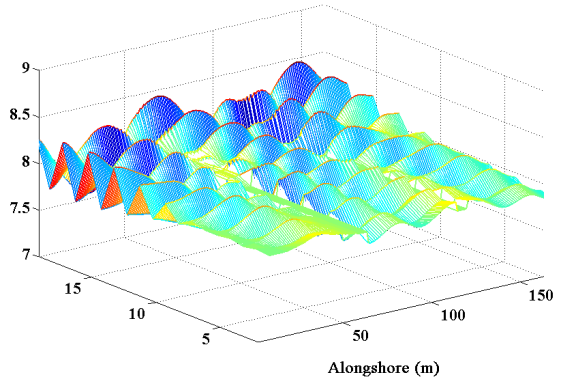

Fig. 11. Wave crest impact in 15 years when wavelength $0.5\sin(t+0.04x)$.

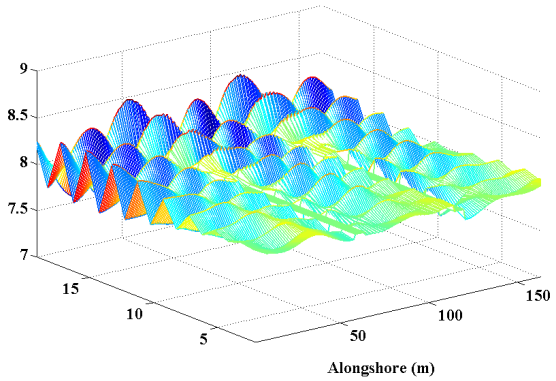

Fig. 12. Wave crest impact in 15 years when wavelength $0.5\sin(t+0.05x)$.

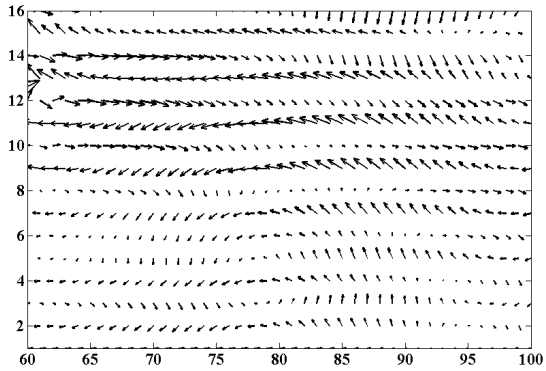

Fig. 13. vector field of velocities between groin when wavelength $0.5\sin(t+0.01x)$.

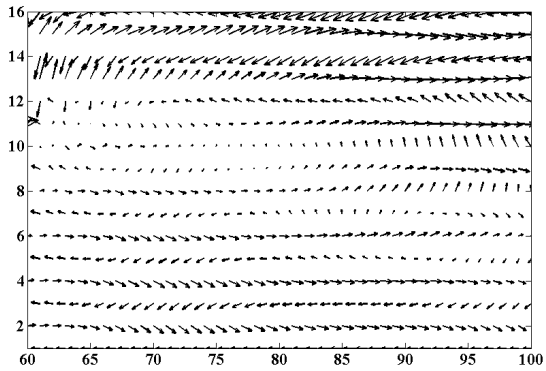

Fig. 14. vector field of velocities between groin when wavelength $0.5\sin(t+0.02x)$.

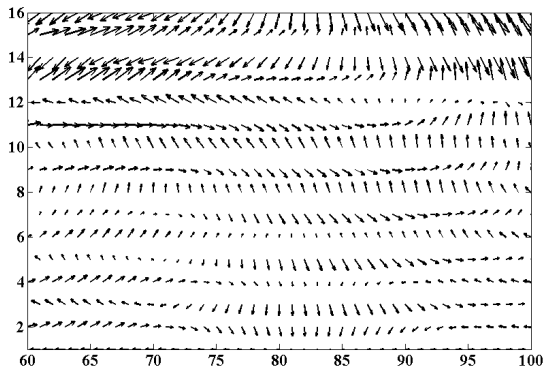

Fig. 15. vector field of velocities between groin when wavelength $0.5\sin(t+0.03x)$.

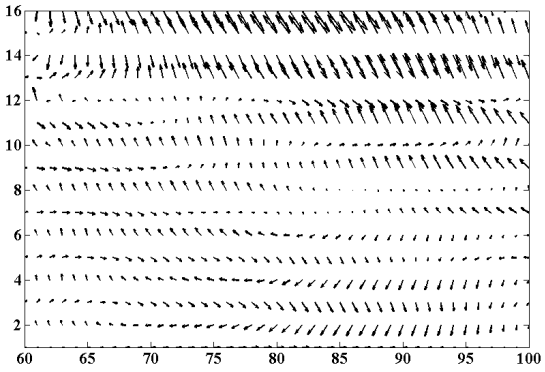

Fig. 16. vector field of velocities between groin when wavelength $0.5\sin(t+0.04x)$.

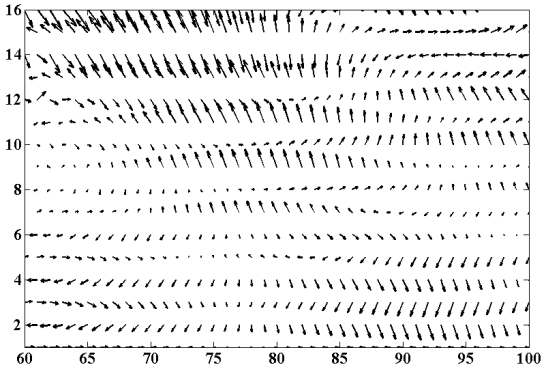

Fig. 17. vector field of velocities between groin when wavelength $0.5\sin(t+0.05x)$.

Table 2-6 shows the averaged wave crest impact (α_0) as obtained by (29).

TABLE II
THE AVERAGED WAVE CREST IMPACT 15 YEARS WHEN WAVELENGTH 1

Time (Years)	Min					
	0-15	15-30	30-45	45-60	60-75	75-90
1	0.0455	0.0448	0.0440	0.0433	0.0426	0.0419
5	-0.0400	-0.0419	-0.0439	-0.0459	-0.0480	-0.0501
10	-0.0705	-0.0721	-0.0737	-0.0754	-0.0770	-0.0786
15	0.0293	0.0284	0.0274	0.0264	0.0254	0.0244
Time (Years)	Distance(m)					
	…	1365-1380	1380-1395	1395-1410	1410-1425	1425-1440
1	…	-0.0379	-0.0394	-0.0410	-0.0426	-0.0442
5	…	-0.0496	-0.1140	-0.1158	-0.1178	-0.1830
10	…	0.1472	0.1363	0.1881	0.1770	0.1658
15	…	0.1930	0.1961	0.1985	0.2003	0.2018

TABLE III
THE AVERAGED WAVE CREST IMPACT 15 YEARS WHEN WAVELENGTH 2

Time (Years)	Min					
	0-15	15-30	30-45	45-60	60-75	75-90
1	0.1817	0.2377	0.2309	0.2241	0.2802	0.2734
5	0.3973	0.4493	0.3794	0.4342	0.4231	0.4109
10	-0.2747	-0.2215	-0.2315	-0.2418	-0.1899	-0.1385
15	-0.0364	-0.0478	0.0037	-0.0077	-0.0191	0.0323
Time (Years)	Distance(m)					
	…	1365-1380	1380-1395	1395-1410	1410-1425	1425-1440
1	…	-0.0275	-0.0380	-0.0485	0.0037	0.0559
5	…	0.1168	0.1154	0.1139	0.1124	0.1109
10	…	-0.1047	-0.1069	-0.1091	-0.1114	-0.1136
15	…	0.2057	0.2040	0.2024	0.2009	0.1993

TABLE IV
THE AVERAGED WAVE CREST IMPACT 15 YEARS WHEN WAVELENGTH 3

Time (Years)	Min					
	0-15	15-30	30-45	45-60	60-75	75-90
1	0.3715	0.3653	0.3595	0.3541	0.3489	0.3440
5	0.1662	0.1767	0.1243	0.1347	0.1449	0.1550
10	0.0148	0.0093	0.0039	-0.0015	-0.0070	-0.0123
15	0.1732	0.1821	0.1910	0.2000	0.2091	0.2182
Time (Years)	Distance(m)					
	…	1365-1380	1380-1395	1395-1410	1410-1425	1425-1440
1	…	0.1182	0.0881	0.1162	0.0782	0.0951
5	…	-0.1423	-0.1392	-0.1361	-0.1330	-0.1300
10	…	0.1488	0.1398	0.1276	0.1550	0.1307
15	…	-0.0660	-0.0623	-0.0586	-0.0550	-0.0514

TABLE V
THE AVERAGED WAVE CREST IMPACT 15 YEARS WHEN WAVELENGTH 4

Time (Years)	Min					
	0-15	15-30	30-45	45-60	60-75	75-90
1	-0.0060	-0.0017	0.0026	0.0068	0.0110	0.0151
5	-0.4238	-0.4291	-0.4346	-0.4403	-0.3833	-0.3894
10	0.3286	0.3249	0.3213	0.3177	0.3142	0.3108
15	-0.4203	-0.4178	-0.4781	-0.4754	-0.4728	-0.4701
Time (Years)	Distance(m)					
	…	1365-1380	1380-1395	1395-1410	1410-1425	1425-1440
1	…	-0.2516	-0.2551	-0.2586	-0.2621	-0.2656
5	…	-0.0892	-0.0940	-0.0360	-0.0408	-0.0454
10	…	0.2663	0.2698	0.2104	0.2139	0.2175
15	…	-0.3283	-0.2725	-0.2801	-0.2880	-0.2960

TABLE VI
THE AVERAGED WAVE CREST IMPACT 15 YEARS WHEN WAVELENGTH 5

Time (Years)	Min					
	0-15	15-30	30-45	45-60	60-75	75-90
1	-0.1214	-0.1405	-0.1557	-0.1691	-0.1188	-0.1310
5	0.1536	0.1497	0.2085	0.2046	0.2006	0.1966
10	-0.0695	-0.0659	-0.0623	-0.0586	-0.0550	-0.0514
15	0.0316	0.0913	0.0882	0.0850	0.0818	0.0786
Time (Years)	Distance(m)					
	…	1365-1380	1380-1395	1395-1410	1410-1425	1425-1440
1	…	0.2402	0.2359	0.2315	0.2271	0.2856
5	…	0.3529	0.3504	0.3479	0.4084	0.4060
10	…	-0.3659	-0.3637	-0.3616	-0.3595	-0.3574
15	…	0.3791	0.3757	0.3723	0.3690	0.3657

V. NUMERICAL EXPERIMENT

In this section, the numerical results of the various beach scenarios are considered and the solution to the idealized problem is introduced. Assuming, during the experiments, that the length of the shoreline considered is L = 100 m and the averaged wave crest impact (α_0) of five case wavelengths. Table 2-6 shows the average wave crest impact of five case wavelengths. Table 7 shows the long-shore transport rate (D) [30]. The simulation setting is illustrated in Fig. 18.

We are going to employ the traditional forward time centered space techniques (15), and the Saulyev finite difference techniques (20), to approximate the shoreline evolution model solution. The approximated solutions are

illustrated in Fig. 19-23. Table 8-17 shows the approximated solutions.

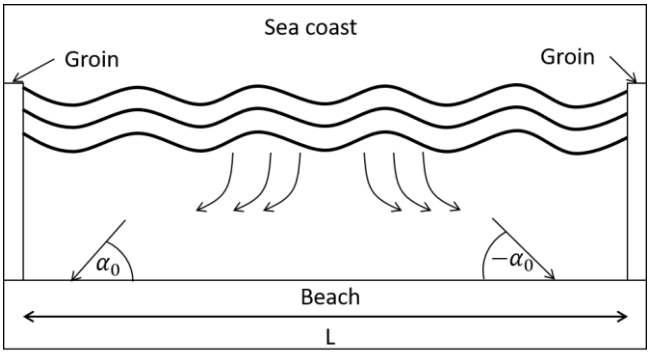

Fig. 18. Initial shoreline.

TABLE VII
THE LONG-SHORE TRANSPORT RATE

Month	$D\ (m/day)$
Jan	79.4659
Feb	62.1307
Mar	5.7869
Apr	61.4403
May	5.6420
Jun	5.4716
Jul	73.0227
Aug	83.071
Sep	121.7301
Oct	372.017
Nov	96.5710
Dec	101.1233

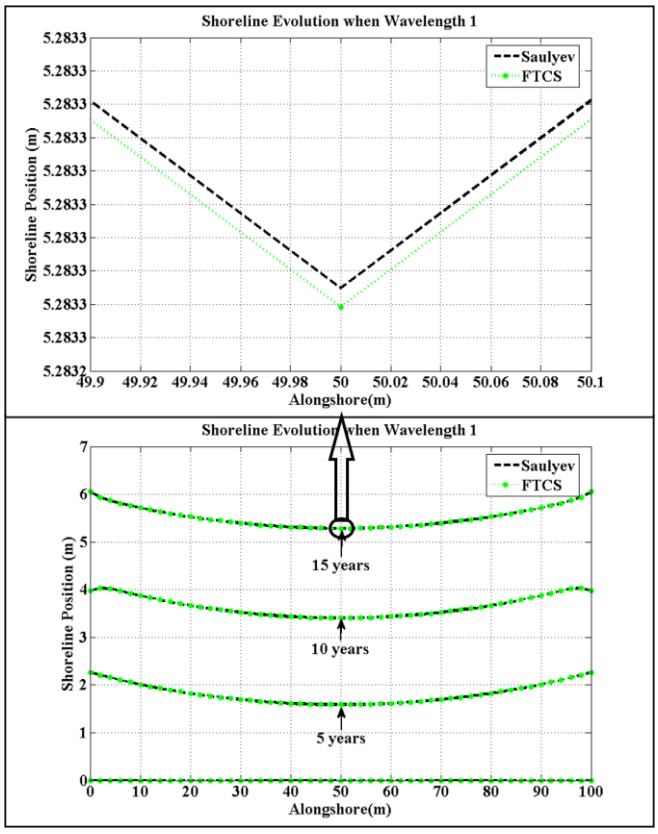

Fig. 19. Shoreline evolution in 15 years when wavelength $0.5\sin(t+0.01x)$.

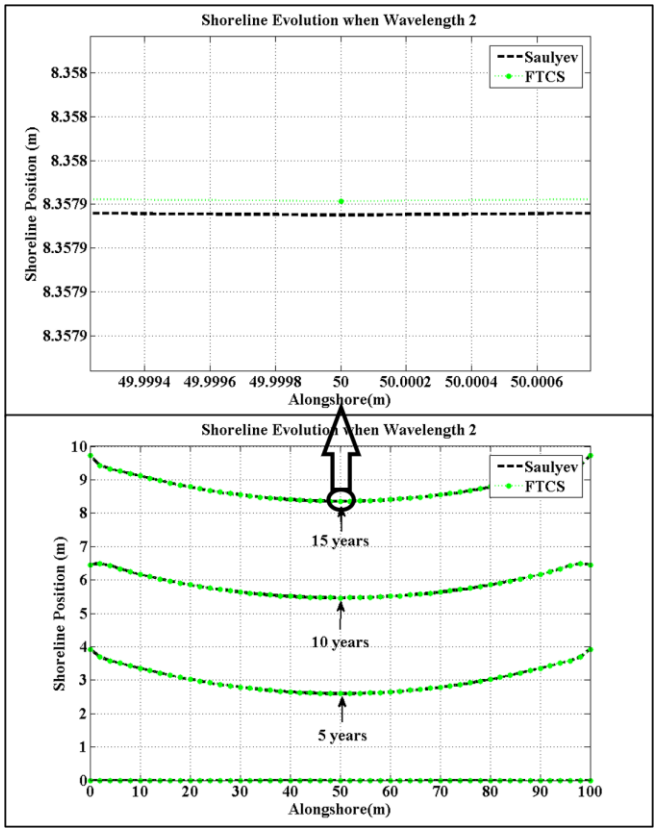

Fig. 20. Shoreline evolution in 15 years when wavelength $0.5\sin(t+0.02x)$.

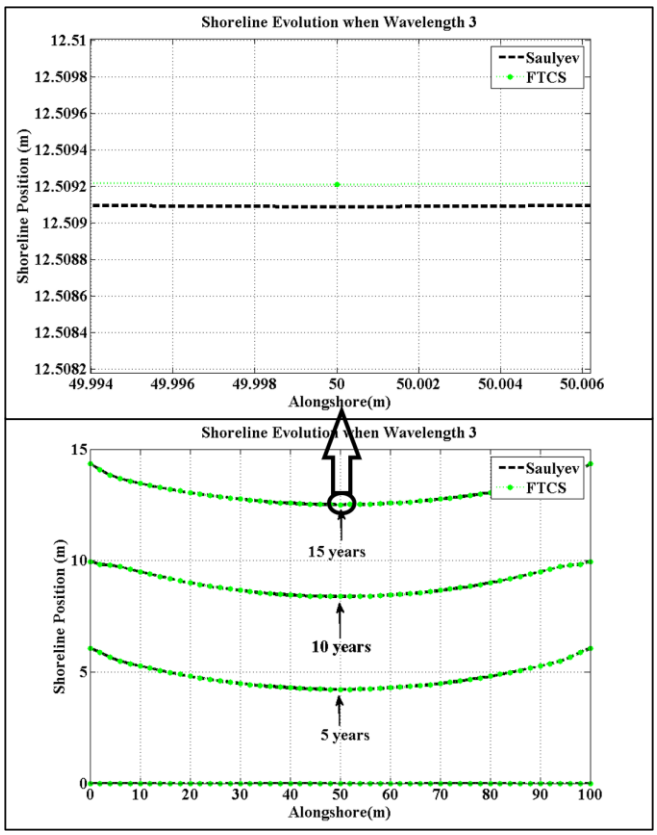

Fig. 21. Shoreline evolution in 15 years when wavelength $0.5\sin(t+0.03x)$.

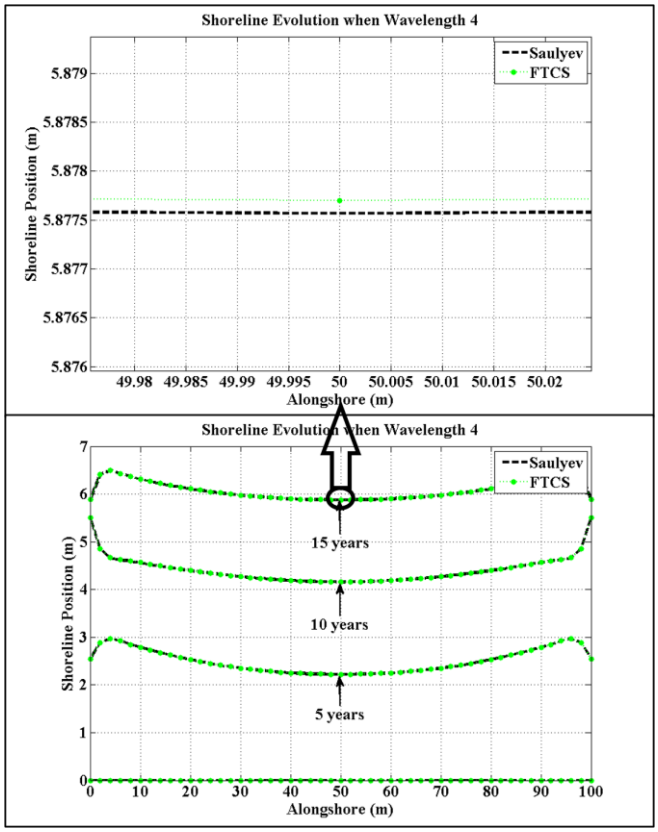

Fig. 22. Shoreline evolution in 15 years when wavelength $0.5\sin(t+0.04x)$.

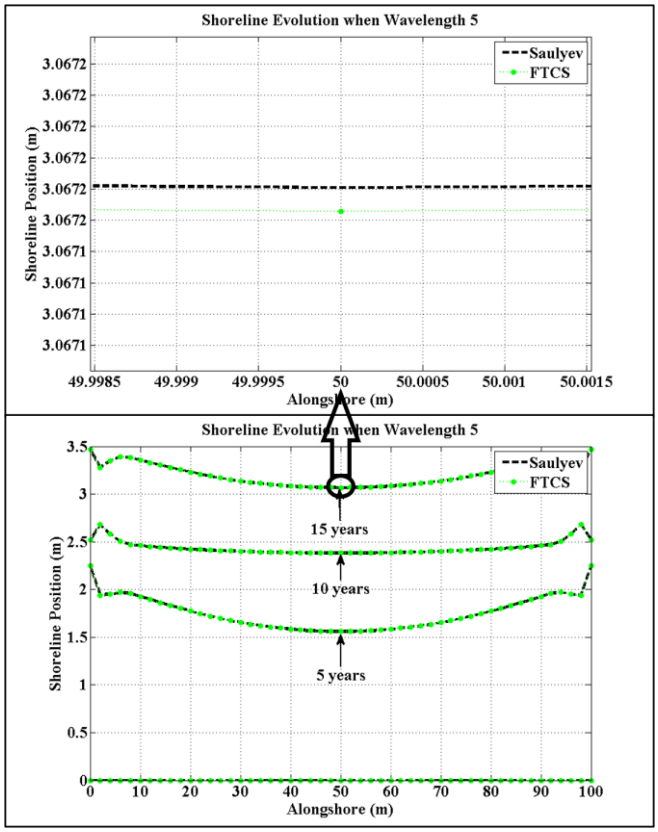

Fig. 23. Shoreline evolution in 15 years when wavelength $0.5\sin(t+0.05x)$.

TABLE VIII
APPROXIMATED SHORELINE EVOLUTION ALONG 15 YEARS USING THE TRADITIONAL FORWARD TIME CENTERED SPACE TECHNIQUES WHEN WAVELENGTH 1

Time (Years)	Distance(m)					
	0	20	40	60	80	100
1	0.8609	0.3967	0.1801	0.1801	0.3967	0.8609
5	2.2665	1.8264	1.6152	1.6152	1.8264	2.2665
10	3.9788	3.6680	3.4335	3.4335	3.6680	3.9788
15	6.0537	5.5284	5.3113	5.3113	5.5284	6.0537

TABLE IX
APPROXIMATED SHORELINE EVOLUTION ALONG 15 YEARS USING THE SAULYEV FINITE DIFFERENCE TECHNIQUES WHEN WAVELENGTH 1

Time (Years)	Distance (m)					
	0	20	40	60	80	100
1	0.8613	0.3969	0.1802	0.1800	0.3965	0.8606
5	2.2662	1.8588	1.6152	1.6152	1.8266	2.2667
10	3.9783	3.6679	3.4334	3.4334	3.6679	3.9788
15	6.0529	5.5280	5.3113	5.3113	5.5285	6.0538

TABLE X
APPROXIMATED SHORELINE EVOLUTION ALONG 15 YEARS USING THE TRADITIONAL FORWARD TIME CENTERED SPACE TECHNIQUES WHEN WAVELENGTH 2

Time (Years)	Distance(m)					
	0	20	40	60	80	100
1	1.2300	0.6412	0.2861	0.2861	0.6412	1.2300
5	3.9256	3.0263	2.6466	2.6466	3.0263	3.9256
10	6.4567	5.8539	5.5070	5.5070	5.8539	6.4567
15	9.7213	8.7855	8.4059	8.4059	8.7855	9.7213

TABLE XI
APPROXIMATED SHORELINE EVOLUTION ALONG 15 YEARS USING THE SAULYEV FINITE DIFFERENCE TECHNIQUES WHEN WAVELENGTH 2

Time (Years)	Distance (m)					
	0	20	40	60	80	100
1	1.2304	0.6416	0.2863	0.2860	0.6409	1.2296
5	3.9260	3.0264	2.6295	2.6466	3.0262	3.9255
10	6.4566	5.8537	5.5068	5.5071	5.8540	6.4568
15	9.7219	8.7857	8.4060	8.4058	8.7853	9.7212

TABLE XII
APPROXIMATED SHORELINE EVOLUTION ALONG 15 YEARS USING THE TRADITIONAL FORWARD TIME CENTERED SPACE TECHNIQUES WHEN WAVELENGTH 3

Time (Years)	Distance(m)					
	0	20	40	60	80	100
1	2.4426	1.0204	0.4643	0.4643	1.0204	2.4426
5	6.0495	4.8087	4.2833	4.2833	4.8087	6.0495
10	9.9512	9.0056	8.4521	8.4521	9.0056	9.9512
15	14.3340	13.0512	12.5716	12.5716	13.0512	14.3340

TABLE XIII
APPROXIMATED SHORELINE EVOLUTION ALONG 15 YEARS USING THE SAULYEV FINITE DIFFERENCE TECHNIQUES WHEN WAVELENGTH 3

Time (Years)	Distance(m)					
	0	20	40	60	80	100
1	2.4427	1.0205	0.4644	0.4641	1.0201	2.4423
5	6.0495	4.8082	4.2831	4.2833	4.8088	6.0495
10	9.9518	9.0062	8.4522	8.4521	9.0054	9.9509
15	14.3339	13.0507	12.5714	12.5715	13.0513	14.3341

TABLE XIV
APPROXIMATED SHORELINE EVOLUTION ALONG 15 YEARS USING THE TRADITIONAL FORWARD TIME CENTERED SPACE TECHNIQUES WHEN WAVELENGTH 4

Time (Years)	Distance(m)					
	0	20	40	60	80	100
1	1.2192	0.6492	0.2962	0.2962	0.6492	1.2192
5	2.5437	2.5297	2.2522	2.2522	2.5297	2.5437
10	5.5018	4.3970	4.1878	4.1878	4.3970	5.5018
15	5.8860	6.1114	5.9015	5.9015	6.1114	5.8860

TABLE XV
APPROXIMATED SHORELINE EVOLUTION ALONG 15 YEARS USING THE SAULYEV FINITE DIFFERENCE TECHNIQUES WHEN WAVELENGTH 4

Time (Years)	Distance (m)					
	0	20	40	60	80	100
1	1.2190	0.6492	0.2962	0.2961	0.6490	1.2189
5	2.5443	2.5302	2.2521	2.2522	2.5295	2.5434
10	5.5016	4.3967	4.1881	4.1879	4.3972	5.5022
15	5.8859	6.1116	5.9013	5.9015	6.1115	5.8859

TABLE XVI
APPROXIMATED SHORELINE EVOLUTION ALONG 15 YEARS USING THE TRADITIONAL FORWARD TIME CENTERED SPACE TECHNIQUES WHEN WAVELENGTH 5

Time (Years)	Distance(m)					
	0	20	40	60	80	100
1	1.1699	0.6231	0.2817	0.2817	0.6231	1.1699
5	2.2472	1.7718	1.5839	1.5839	1.7718	2.2472
10	2.5173	2.4222	2.3866	2.3866	2.4222	2.5173
15	3.4696	3.2305	3.0839	3.0839	3.2305	3.4696

TABLE XVII
APPROXIMATED SHORELINE EVOLUTION ALONG 15 YEARS USING THE SAULYEV FINITE DIFFERENCE TECHNIQUES WHEN WAVELENGTH 5

Time (Years)	Distance(m)					
	0	20	40	60	80	100
1	1.1701	0.6235	0.2819	0.2816	0.6226	1.1696
5	2.2477	1.7722	1.5840	1.5837	1.7713	2.2466
10	2.5165	2.4214	2.3861	2.3865	2.4226	2.5175
15	3.4704	3.2312	3.0841	3.0837	3.2299	3.4691

We will compare the five wavelengths with time durations of 5, 10, and 15 years, as illustrated in Fig. 24-27.

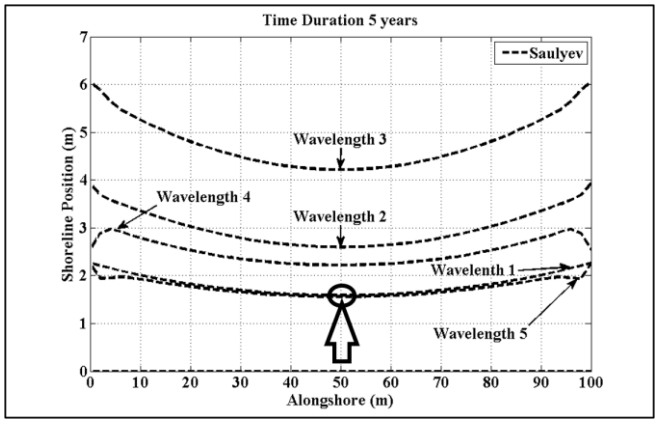

Fig. 24. Wavelength Comparisons in 5 years.

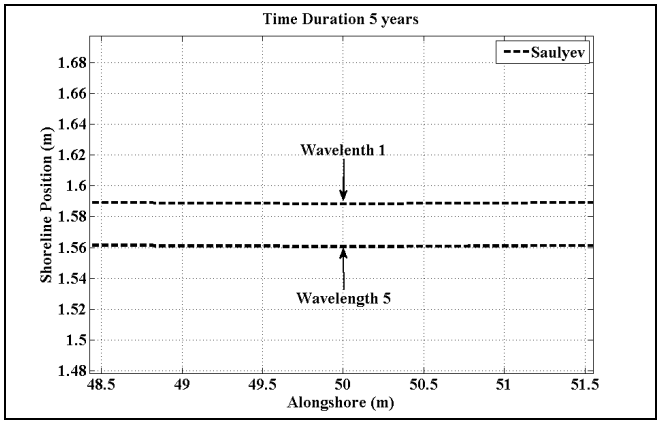

Fig. 25. Enlarge Between Wavelength 1 and Wavelength 5 at 50 m.

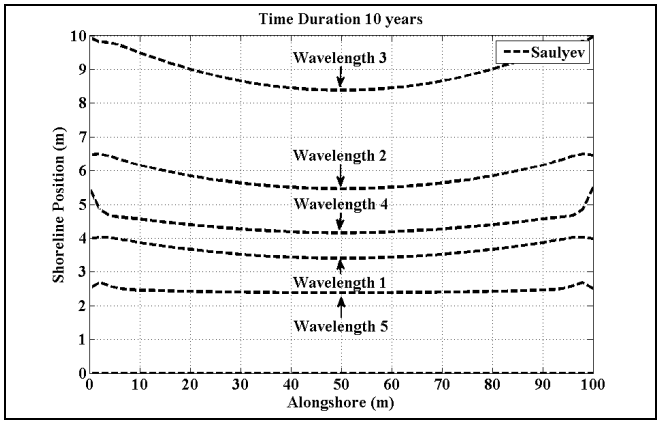

Fig. 26. Wavelength Comparisons in 10 years.

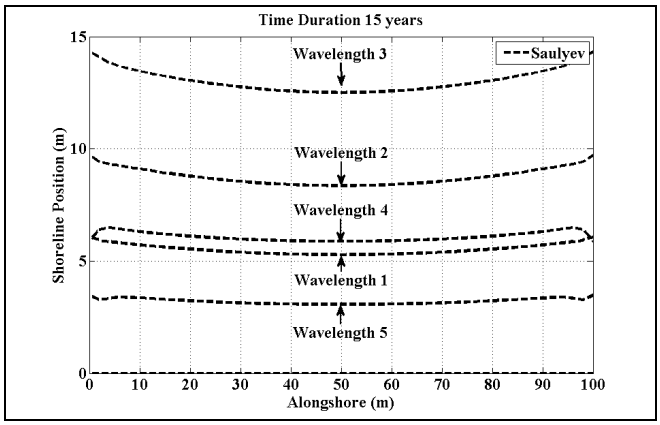

Fig. 27. Wavelength Comparisons in 15 years.

VI. DISCUSSION

In this paper, we considered the averaged wave crest impact (α_0) as obtained by (29) for five case wavelengths as seen in Table 2-6. The long-shore transport rate (D) for each month as seen in Table 7.

We used the numerical method, the traditional forward time centered space techniques, and the Saulyev finite difference techniques to predict the shoreline evolution for five case wavelengths with time duration of 5, 10, and 15 years.

The approximated shoreline evolution for wavelength $0.5\sin(t+0.01x)$ with a time duration of 15 years is seen in Table 8, 9, and Fig. 19. The farthest distance from the shoreline evolution is 6.0537 m. The shortest distance from the shoreline evolution is 5.2833 m.

The approximated shoreline evolution for wavelength $0.5\sin(t+0.02x)$ with a time duration of 15 years is seen in Table 10, 11, and Fig. 20. The farthest distance from the shoreline evolution is 9.7219 m. The shortest distance from the shoreline evolution is 8.3579 m.

The approximated shoreline evolution for wavelength $0.5\sin(t+0.03x)$ with a time duration of 15 years is seen in Table 12, 13, and Fig. 21. The farthest distance from the shoreline evolution is 14.3339 m. The shortest distance from the shoreline evolution is 12.5092 m.

The approximated shoreline evolution for wavelength $0.5\sin(t+0.04x)$ with a time duration of 15 years is seen in Table 14, 15, and Fig. 22. The farthest distance from the shoreline evolution is 6.4928 m. The shortest distance from the shoreline evolution is 5.8776 m.

The approximated shoreline evolution for wavelength $0.5\sin(t+0.05x)$ with a time duration of 15 years is seen in Table 16, 17, and Fig. 23. The farthest distance from the shoreline evolution is 3.4704 m. The shortest distance from the shoreline evolution is 3.0672 m.

The approximated shoreline evolution for five case wavelengths with time durations of 5, 10, and 15 years is seen in Fig 24, 25, 26, and 27 respectively.

The approximated shoreline evolutions of both numerical approaches within five wavelengths of the considered shoreline are compatible.

VII. Conclusion

A more realistic shoreline evolution model was created in this research to adjust for the wavelength influence of breaking waves on groin construction. The initial condition setting approach and boundary conditions techniques, as well as various groin structural impacts, are discussed. Each year, the shoreline evolution is approximated using the conventional forward time centered space method and the unconditionally stable Saulyev finite differential methods. The estimated impacts of shoreline evolution were consistent with the wave crest impact model for five case wavelengths. As a result, the frequency of the wavelength influences the approximated shoreline evolution rate. In most cases, when the frequency of wavelength increases, the approximated shoreline evolution that obtains shoreline area also increases, but in some cases, when the frequency of wavelength increases, the approximated shoreline evolution has shoreline area obtained less. The approximated shoreline evolution is uncertain at different frequencies of wavelengths. The proposed modeling could be used to forecast the effectiveness of constructing a groin system on a nearby beach.

References

[1] H. Hanson, N. C. Kraus, and S. H. Blomgren, "Modern functional design of groin systems," Coastal Engineering, pp. 1327–1342, 1994.

[2] S. Krishna Prasad, K. P. Indulekha, and K. Balan, "Analysis of groyne placement on minimising river bank erosion," Procedia Technology, vol. 24, pp. 47–53, 2016.

[3] W. T. Bakker, "The dynamics of coast with a groin system," Proceeding of 11th Coastal Engineering Conference 1969, pp. 492–517.

[4] W. T. Bakker, and T. Edelman, "The coastline of river deltas," Proceeding of 9th Coastal Engineering Conference 1965, pp. 199–218.

[5] W. Grijimr, "Theoretical form of shoreline," Proceeding of 7th Coastal Engineering Conference 1961, pp. 197–202.

[6] W. Grijimr, "Theoretical form of shoreline," Proceeding of 9th Coastal Engineering Conference 1965, pp. 219–235.

[7] B. Le Mahute, and M. Soldate, "Mathematical Modeling of Shoreline Evolution," US Army Corps of Engineer Waterways Experiment Station, CERC, 1977.

[8] T. Waltonand, and T. Chiu, "A review of analytical technique to solve the sand transport equation and some simplified solution," Coastal Structure, pp. 809–837, 1979.

[9] H. Hanson, M. Larson, and N. C. Kraus, "Analytical Solution of the One-line Model for Shoreline Changel," US Army Corps of Engineer Waterways Experiment Station, CERC, 1987.

[10] US Army Corp of Engineers, "Shore Protection Manual," Coastal Engineering Research Centre, Washington, 1984.

[11] L. X. Hoan, "Some result of comparison between numerical and analytical solutions of the one-line model for shoreline change," Vietnam Journal of Mechanics., pp. 94–102, 2006.

[12] M. Mamat Subiyanto, M. F. Ahmad, and M. L. Husain, "Comparison of numerical method for forward and backward time centered space for long – term simulation of shoreline evolution," Applied Mathematical Sciences, vol. 7, pp. 5165–5173, 2013.

[13] N. Pochai, "Unconditional stable numerical techniques for a water-quality model in a non-uniform flow stream," Advances in Difference Equations, vol. 2017, Article ID 286, 13 pages, 2017.

[14] P. Samalerk, and N. Pochai, "Numerical Simulation of a One-Dimensional Water-Quality Model in a Stream Using a Saulyev Technique with Quadratic Interpolated Initial-Boundary Conditions," Abstract and Applied Analysis, vol. 2018, Article ID 1926519, 7 pages, 2018.

[15] Ben Wongsaijai, Kanyuta Poochinapan, and Thongchai Disyadej, "A Compact Finite Difference Method for Solving the General Rosenau-RLW Equation," IAENG International Journal of Applied Mathematics, vol. 44, no. 4, pp. 192-199, 2014.

[16] Shixiang Zhou, Fanwei Meng, Qinghua Feng, and Li Dong, "A Spatial Sixth Order Finite Difference Scheme for Time Fractional Sub-diffusion Equation with Variable Coefficient," IAENG International Journal of Applied Mathematics, vol. 47, no. 2, pp. 175-181, 2017.

[17] Kewalee Suebyat, and Nopparat Pochai, "A Numerical Simulation of a Three-dimensional Air Quality Model in an Area Under a Bangkok Sky Train Platform Using an Explicit Finite Difference Scheme," IAENG International Journal of Applied Mathematics, vol. 47, no. 4, pp. 471-476, 2017.

[18] Alia Khurram, and David W Kammler, "Numerical Generation of Images for the Gibbs Phenomenon Near a Corner in the Plane," IAENG International Journal of Applied Mathematics, vol. 44, no. 1, pp. 15-22, 2014.

[19] Tata Sutardi, Linwei Wang, Manosh C. Paul, and Nader Karimi, "Numerical Simulation Approaches for Modelling a Single Coal Particle Combustion and Gasification," Engineering Letters, vol. 26, no. 2, pp. 257-266, 2018.

[20] Linna Li, Zhirou Wei, and Qiongdan Huang, "A Numerical Method for Solving Fractional Variational Problems by the Operational Matrix Based on Chelyshkov Polynomials," Engineering Letters, vol. 28, no. 2, pp. 486-491, 2020.

[21] Witsarut Kraychang, and Nopparat Pochai, "A Simple Numerical Model for Water Quality Assessment with Constant Absorption around Nok Phrao Island of Trang River," Engineering Letters, vol. 28, no. 3, pp. 912-922, 2020.

[22] Elvira Armenio, Francesca De Serio, Michele Mossa, and Antonio F. Petrillo, "Coastline evolution based on statistical analysis and modeling," Nat. Hazards Earth Syst. Sci., 19, pp. 1937–1953, 2019.

[23] C. Coelho, F. Celoso-Gomes, and R. Silva, "Shoreline coastal evolution model: two Portuguese case studies," Coastal Engineering, vol. 5, pp. 3430-3441, 2006.

[24] J. Guillen, M. J. F. Stive, and M. Capobianco, "Shoreline evolution of the holland coast on a decadal scale," Earth Surface Processes and Landforms, vol. 24, pp. 517-536, 1999.

[25] P. K. Mohanty, S. K. Patra, W. Bramha, B. Seth, U. Pradhan, B. Behera, P. Mishra, and U. S. Panda, "Impact of Groins on Beach Morphology: A Case Study near Gopalpur Port, East Coast of India," Journal of Coastal Research, vol. 28, pp. 132-142, 2012.

[26] Laura Lemke, J. K. Miller, A. Gorton, and E. Livermont, "EOF Analysis of Shoreline Changes Following an Alternative Beachfill within a Groin Field," Coastal Engineering Proceedings 2014, 12 pages, 2014.

[27] Le Xuan Roan, "Some results of comparison between numerical and analytic solutions of the one-line model for shoreline change," Vietnam Journal of Mechanics, VAST, vol. 28, pp. 94-102, 2006.

[28] Witsarut Kraychang and Nopparat Pochai, “Numerical Treatment to a Water-Quality Measurement Model in an Opened-Closed Reservoir,” Thai Journal of Mathematics, vol. 13, pp. 775-788, 2015.
[29] A. R. Mitchell, “Computational Methods in Partial Differential Equations,” John Wiley & Sons Ltd., London, 1969.
[30] Pidok Unyapoti and Nopparat Pochai, “A Shoreline Evolution Model with a Twin Groins Structure using Unconditionally Stable Explicit Finite Difference Techniques.” Engineering Letters, vol. 29, no. 1, pp. 288-296, 2021.
[31] Pidok Unyapoti and Nopparat Pochai, “A One-Dimensional Mathematical Model of Long-Term Shoreline Evolution with Groin System using an Unconditionally Stable Explicit Finite Difference Method,” International Journal of Simulation: Systems, Science and Technology, vol. 21, no.3, pp. 2.1-2.6, 2020.
[32] W. Kraychang, S. Meechowna, W. Welamas, and N. Pochai, "A Simple Mathematical Model of Water Quality Control for Recirculating Pond on A Shrimp Farm," Engineering Letters, vol 24, no 4, pp. 1470 – 1477, 2021.
[33] Pornpon Othata and Nopparat Pochai, "A Mathematical Model of Salinity Control in a River with an Effect of Internal Waves using Two Explicit Finite Difference Methods," Engineering Letters, vol 29, no 2, pp.689-696, 2021.
[34] Piyada Phosri and Nopparat Pochai, "A Couple Mathematical Models of the Water Quality Measurement in a Stream using Upwind Implicit Methods," IAENG International Journal of Applied Mathematics, Vol.51, No.1, pp. 237-249, 2021

N. Pochai is a researcher of Centre of Excellence in Mathematics, MHESI, Bangkok 10400, Thailand.

P. Unyapoti is an assistant researcher of Centre of Excellence in Mathematics, MHESI, Bangkok 10400, Thailand.